RESEARCH MEMORANDUM

for the

Bureau of Aeronautics, Department of the Navy

ROUGH-WATER LANDINGS OF A $\frac{1}{10}$-SIZE POWERED DYNAMIC MODEL OF THE XP5Y-1 FLYING BOAT WITH TWO TYPES OF AFTERBODY - LANGLEY TANK MODEL 228

TED NO. NACA DE309

By

Charlie C. Garrison

Langley Aeronautical Laboratory
Langley Air Force Base, Va.

NATIONAL ADVISORY COMMITTEE
FOR AERONAUTICS

WASHINGTON

NATIONAL ADVISORY COMMITTEE FOR AERONAUTICS

RESEARCH MEMORANDUM

for the

Bureau of Aeronautics, Department of the Navy

ROUGH-WATER LANDINGS OF A $\frac{1}{10}$-SIZE POWERED DYNAMIC MODEL OF THE XP5Y-1 FLYING BOAT WITH TWO TYPES OF AFTERBODY - LANGLEY TANK MODEL 228

TED NO. NACA DE309

By Charlie C. Garrison

SUMMARY

A $\frac{1}{10}$-size powered dynamic model of a large, high-speed flying boat was landed in Langley tank no. 1 into oncoming waves 4 feet high (full size). The model was tested with two afterbodies of differing lengths (4.12 and 6.63 beams). The short afterbody had a constant angle of dead rise of $22\frac{1}{2}^\circ$ and a keel angle of 6.5°. The long afterbody had warped dead rise and a keel angle of 8.5°.

The vertical accelerations were slightly greater and the maximum angular accelerations and maximum trims were slightly less for the model with the long afterbody than for the model with the short afterbody. A wave length of 210 feet (full size) imposed the highest accelerations on the model with either the long or the short afterbody.

INTRODUCTION

At the request of the Bureau of Aeronautics, Department of the Navy, the landing behavior in rough water of a $\frac{1}{10}$-size powered dynamically-similar model of the Convair XP5Y-1 flying boat was investigated in Langley tank no. 1. The tests were made in July and September 1947. At that time the XP5Y-1 had a gross weight of 125,000 pounds, a wing loading of 59.5 pounds per square foot and a power loading of 9.5 pounds per horsepower.

The model was tested with two types of afterbody which differed principally in length, but which also differed somewhat in keel angle and dead rise variation. All the landings were made into oncoming waves.

DESCRIPTION OF MODELS

The general arrangement of the model with the basic afterbody is shown in figure 1, this configuration being designated Langley tank model 228D. The basic afterbody was 4.12 beams in length, had a constant angle of dead rise of $22\frac{1}{2}^\circ$, and a keel angle of 6.5°. The other afterbody was 6.63 beams in length and had a keel angle of 8.5°. The angle of dead rise (fig. 2) was 28° at the step, increased to a maximum $36\frac{1}{2}^\circ$ at approximately 2 beams aft of the step, and then decreased to about 25° at the sternpost. The model with the long afterbody was designated model 228F. The two afterbodies are compared in figure 2.

The depth of step used with each afterbody was selected as the minimum depth of step, which resulted in adequate landing stability in smooth water. (See reference 1.) Models 228D and 228F are identical, respectively, with models 228D-15.0 and 228F-21.8 in reference 1, the abbreviated designations being used for simplicity.

The model and the two afterbodies were supplied by the Consolidated Vultee Aircraft Corporation. Table I gives the pertinent dimensions of the model and the airplane assumed for the tests.

Full-span leading-edge slats were added to the wing of the model as shown in figure 1. These slats compensate for the early stall and low maximum lift coefficient experienced at the low Reynolds numbers at which the tests were run.

APPARATUS AND PROCEDURE

The tank and towing carriage are described in reference 2. The models were fixed in roll and yaw but were free to trim about the pivot which was located at the center of gravity and were free to move vertically. The roller cage carrying the towing staff was free to move a short distance fore and aft, so that with a suitable combination of model thrust (approximately one-half take-off power) and carriage deceleration (3 ft/sec^2), the models were practically free of longitudinal restraint during the most severe part of the landing run-out.

During each landing time-history records were obtained on a recording oscillograph. The vertical location of the center of gravity,

the trim, and the fore-and-aft movements of the model relative to the towing carriage were recorded by means of electrical slide-wire bridges connected to the oscillograph. The profile of the waves and the speed of the towing carriage were recorded, and electrical contacts located flush with the keel at the bow, step, and sternpost registered deflections on the record when these points entered and left the water. The vertical accelerations were measured by means of an accelerometer mounted on the staff. The angular accelerations were measured by means of a pair of linear accelerometers mounted inside the model and connected electrically to give a single output which was proportional to the angular acceleration. All three accelerometers were an oil damped strain-gage type. The output signals from the accelerometers were fed to recording galvanometers, which had natural frequencies of about 35 cycles per second and were damped to approximately 0.7 of the critical value.

The waves were about 5 inches high (4 feet, full size) and 14, 21, 26, and 31 feet long (140, 210, 260, and 310 feet, respectively, full size). The shortest regular wave that could be generated at the water level used for these tests was 14 feet in length. Since the position on the wave at which the model landed was not controlled, several landings were made in each wave to insure that impacts near the maximum severity would be attained. The tests of reference 3 indicated that for landing trims above 4° there was no appreciable effect of the initial landing trim on either the variation of trim during the run-out or the maximum vertical acceleration. All landings in the present investigation, therefore, were made at an initial trim of approximately 10°.

In general, the landing procedure was similar to that described in reference 1. The towing carriage was accelerated until the model was air-borne. The model was trimmed to approximately 10° by use of the elevators, and an electrically-operated trim brake was set. The elevators were adjusted so that the model would be in trim just prior to contact with the water; the carriage was then decelerated at a rate of approximately 3 feet per second per second (0.1g), and the model was allowed to land. The brake was released automatically when the model contacted any part of a wave, and the model was free to trim during the run-out. The propeller thrust was adjusted so that the resultant horizontal force was approximately zero at contact with the water. The model, therefore, was free to move fore and aft throughout most of the landing run.

All landings were made with the center of gravity at 30 percent mean aerodynamic chord and with the flaps deflected 50° (gaps sealed).

RESULTS

The maximum vertical acceleration and maximum angular acceleration measured during the first impact of each landing run and the maximum trim resulting from the first impact are presented in figures 3(a)

and 3(b) for models 228D and 228F, respectively. The maximum vertical acceleration, maximum angular acceleration, and maximum trim measured during each landing run are plotted in figure 4.

A comparison of the trims and accelerations during initial impact for the two models is presented in figure 5. The maximum accelerations and maximum trims encountered during landings are compared for both models in figure 6.

The sinking speeds and flight-path angles measured at initial contact are plotted against the vertical accelerations during initial impact in figure 7. The same quantities measured at maximum vertical acceleration are plotted against the maximum vertical acceleration in figure 8.

All of the results are presented as full-size values.

DISCUSSION

The motions of both models appeared quite violent during nearly all of the landings. For a given height of wave, the vertical and angular accelerations and maximum trims (figs. 3 and 4) increased as the wave length was decreased to a length of approximately 210 feet. At shorter wave lengths than 210 feet the accelerations and maximum trims again decreased. This critical wave length (wave length where the maximum acceleration occurred) was approximately the same for both models, approximately twice the length of the planing bottom for model 228D and one and one half times the length of the planing bottom for model 228F.

The comparisons of figures 5 and 6 show that the vertical accelerations for the model with the long afterbody, model 228F, reached slightly higher maximums than those for the model with the short afterbody. This result was opposite to that described in references 3 and 4, where it was shown that an increase in length of afterbody reduced the vertical accelerations (dead rise and keel angle remaining unchanged). The afterbodies of the present model, however, differed in keel angle and dead rise as well as length, and apparently the influences of these differences were sufficient to overshadow the effect of length alone. The maximum trim attained as a result of planing off the waves, however, was less for the model with the long afterbody than for the model with the short afterbody. The angular accelerations were higher during first impact and lower at worst impact for the model with the long afterbody.

The sinking speed and flight-path angle were not directly controllable during any impact, but figure 7 indicates that, for initial impacts, the sinking speed was approximately 5.0 feet per second (300 feet per minute) and the flight-path angle was about 2°. At maximum vertical acceleration, the sinking speed varied from approximately 10 to 20 feet per second (600 to 1200 feet per minute) and the flight-path angles

ranged from about 6° to 12° for model 228D and from about 4° to 10° for model 228F, figure 8.

Extremely heavy spray was observed to strike the horizontal tail surfaces during landings of the model with the short afterbody. This spray condition was much less severe with the long afterbody.

CONCLUSIONS

1. Maximum vertical and angular accelerations and maximum trim occurred on landings made in waves 210 feet long when either afterbody was used.

2. The maximum vertical accelerations were slightly higher and the maximum trims were lower for the model with the long afterbody than for the model with the short afterbody.

Langley Aeronautical Laboratory
National Advisory Committee for Aeronautics
Langley Air Force Base, Va.

Norman A. Land
for
Charlie C. Garrison
Aeronautical Research Scientist

Approved:

John B. Parkinson
Chief of Hydrodynamics Division

jjm

REFERENCES

1. Garrison, Charlie C., and Clement, Eugene P.: Tank Tests of Three Types of Afterbodies on a Flying-Boat Model with Basic Hull Length-Beam Ratio of 10.0. NACA TN No. 1547, 1948.

2. Truscott, Starr: The Enlarged N.A.C.A. Tank, and Some of Its Work. NACA TM No. 918, 1939.

3. Benson, James M., Havens, Robert F., and Woodward, David R.: Landing Characteristics in Waves of Three Dynamic Models of Flying Boats. NACA RM No. L6L13, 1946.

4. Carter, Arthur W.: Effect of Hull Length-Beam Ratio on the Hydrodynamic Characteristics of Flying Boats in Waves. NACA TN No. 1782, 1949.

TABLE I

AERODYNAMIC AND PROPULSIVE CHARACTERISTICS AND HULL DIMENSIONS OF LANGLEY TANK MODEL 228 AND FULL-SIZE FLYING BOAT

	$\frac{1}{10}$-size model	Full-size flying boat
Design gross load	123.5	125,000
Gross load coefficient, C_{Δ_o}	1.95	1.95
Wing area, sq ft	21.0	2,100
Take-off horsepower	4.17	13,200
Wing loading, lb/sq ft	5.88	59.5
Power loading, lb/hp	29.6	9.47
Over-all length, in.	151.7	1517.0
Location of centroid of step, percent M.A.C.	36.1	36.1
Height of center of gravity above base line, in.	17.2	172.1
Wing:		
Span, in.	174	1,740
Angle of wing setting to base line, deg	5.0	5.0
Mean aerodynamic chord (M.A.C.), in.	18.9	189
Leading edge M.A.C.		
Aft of bow, in.	63.7	637
Above base line, in.	22.2	222
Flaps (slotted)		
Take-off deflection, deg	20	20
Landing deflection, deg	50	50
Horizontal tail surfaces:		
Span, in.	66.4	664
Leading edge at root		
Aft of bow, in.	130.36	1303.6
Above base line, in.	24.83	248.3
Angle of stabilizer to base line, deg	-1.0	-1.0
Dihedral, deg	10.0	10.0
Propellers:		
Number	4	4
Blades	4	4
Diameter, in.	18.1	181
Blade angle (3/4 radius), deg	10.0	10.0
Revolutions per minute with full power	5250	-------
Angle of thrust line to base line, deg	2.0	2.0

TABLE I

AERODYNAMIC AND PROPULSIVE CHARACTERISTICS AND HULL DIMENSIONS OF LANGLEY TANK MODEL 228 AND FULL-SIZE FLYING BOAT - Concluded

	$\frac{1}{10}$-size model	Full-size flying boat
Forebody of hull:		
Maximum beam, in.	12.0	120
Length from bow to centroid of step, in.	70.49	704.9
Length-beam ratio	5.87	5.87
Angle of step (V-type), deg	30	30
Angle of forebody keel to base line, deg	0	0
Angle of dead rise at step, deg		
Excluding chine flare	22.5	22.5
Including chine flare	18.0	18.0
Extent of constant dead rise from centroid of step, beams	3/4	3/4
Constant-dead rise afterbody:		
Length from centroid of step to sternpost, in.	49.51	495.1
Length-beam ratio	4.13	4.13
Angle of afterbody keel, deg	6.5	6.5
Angle of dead rise, deg	22.5	22.5
Depth of step at centroid, percent beam	15.0	15.0
Extended warped-dead rise afterbody:		
Length from centroid of step to sternpost, in.	79.61	796.1
Length-beam ratio	6.63	6.63
Angle of afterbody keel, deg	8.5	8.5
Depth of step at centroid, percent beam	21.8	21.8

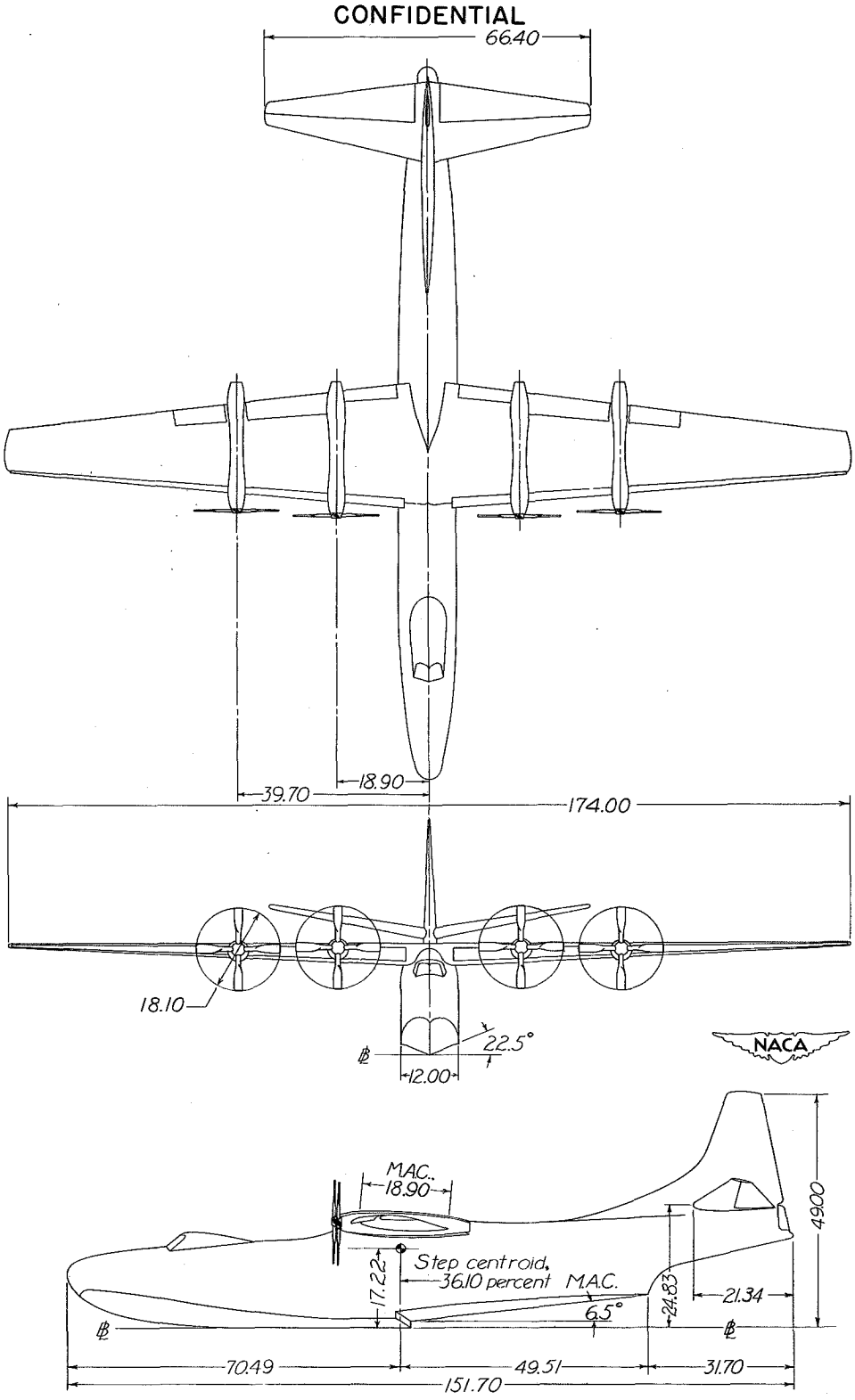

Figure 1.- General arrangement of Langley tank model 228D.
(Dimensions are in inches.)

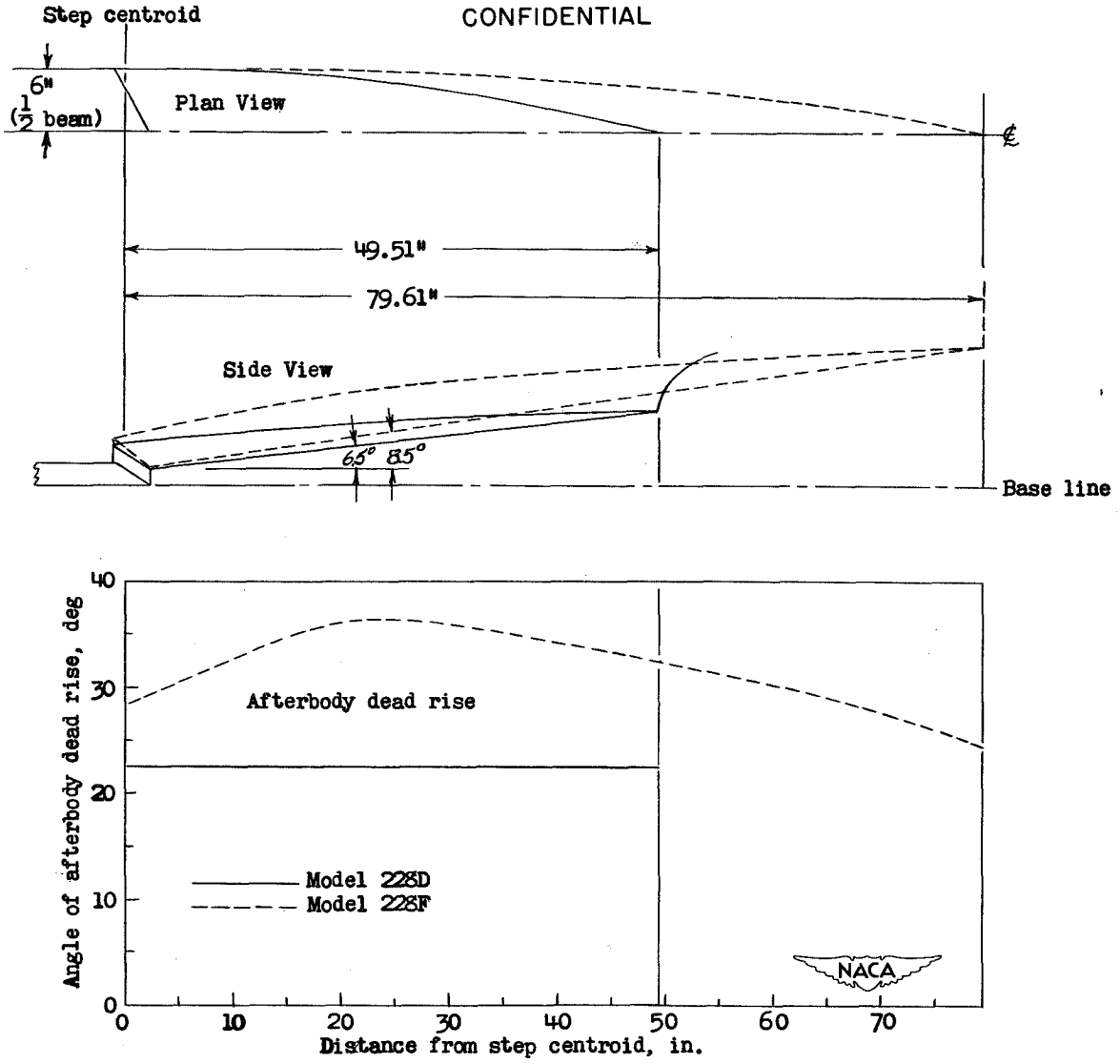

Figure 2.- The two afterbodies tested on model 228.

CONFIDENTIAL

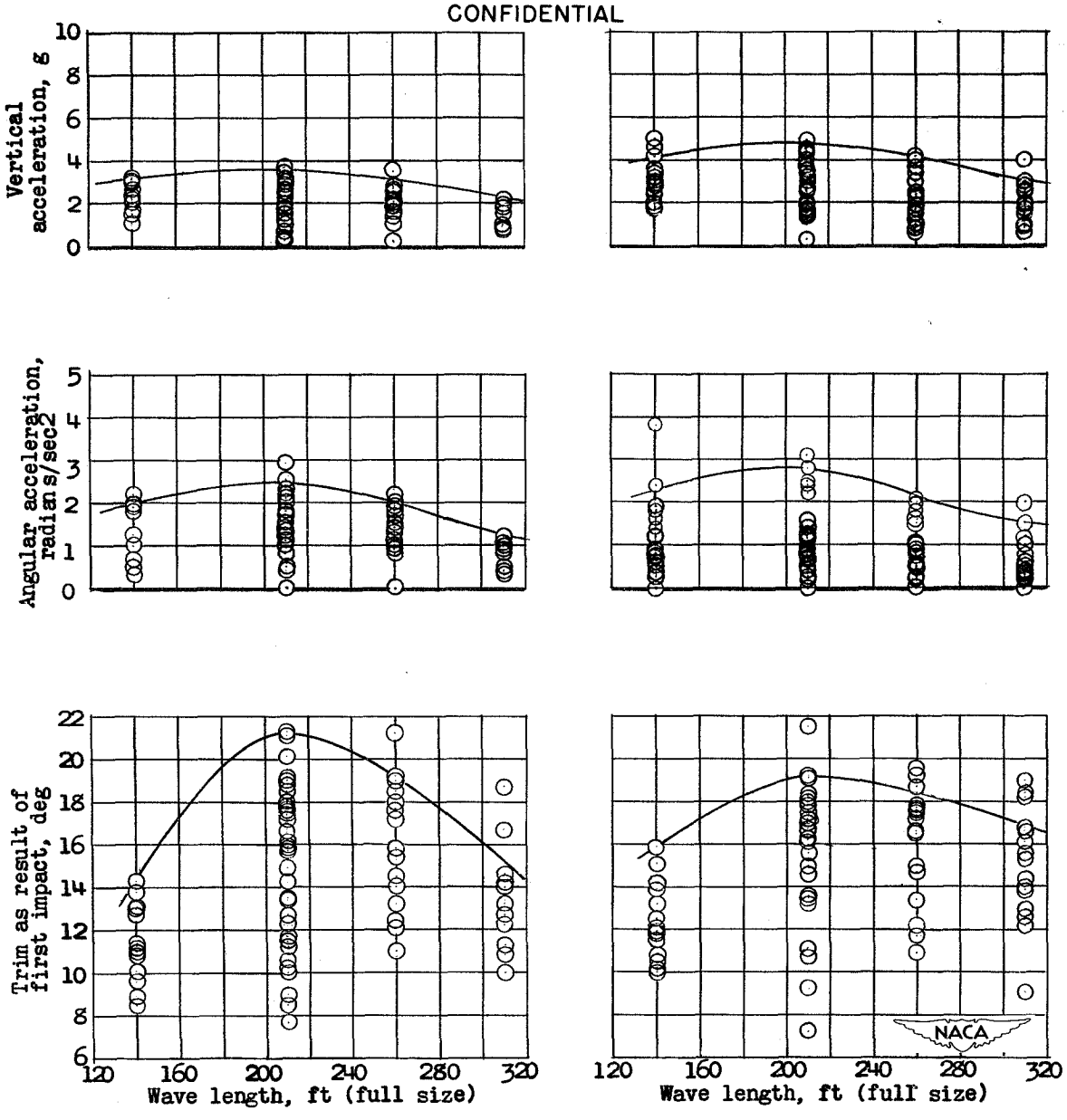

(a) Model 228D. (b) Model 228F.

Figure 3.- Variation of accelerations and trim with wave length during first impact.

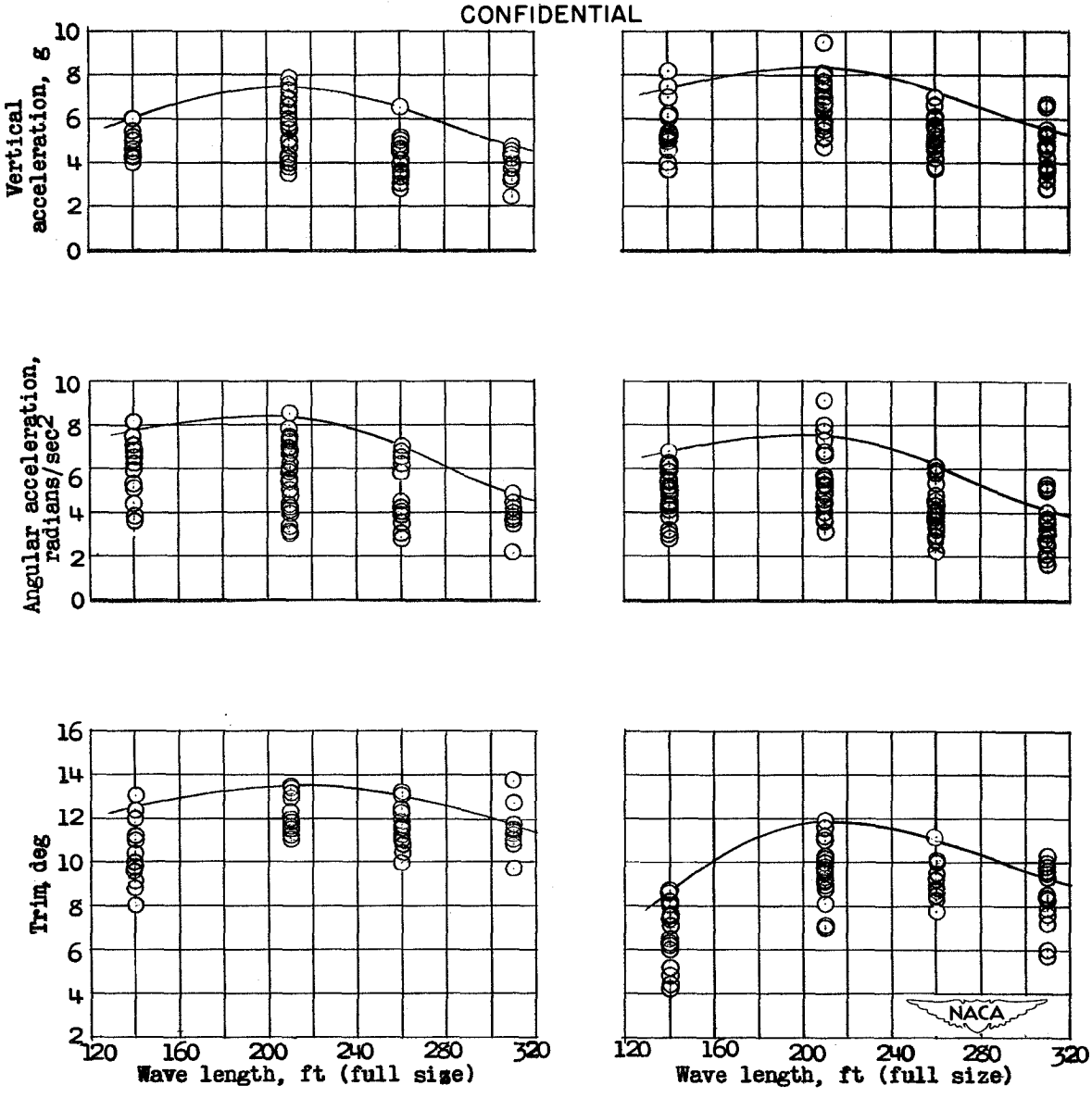

(a) Model 228D.

(b) Model 228F.

Figure 4.- Maximum accelerations and trims during landing run-out.

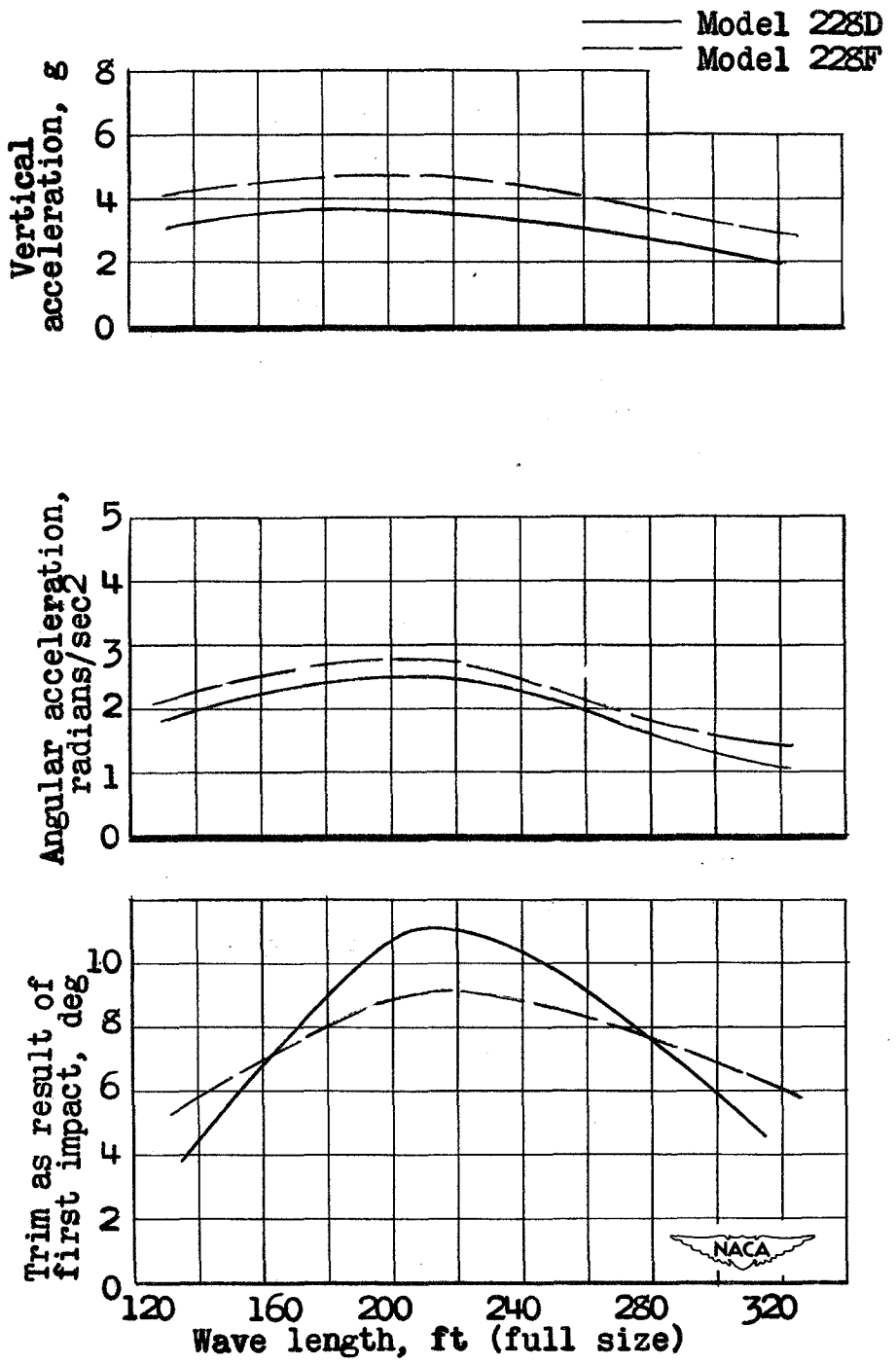

Figure 5.- Comparison of accelerations and trim during first impacts of models 228D and 228F.

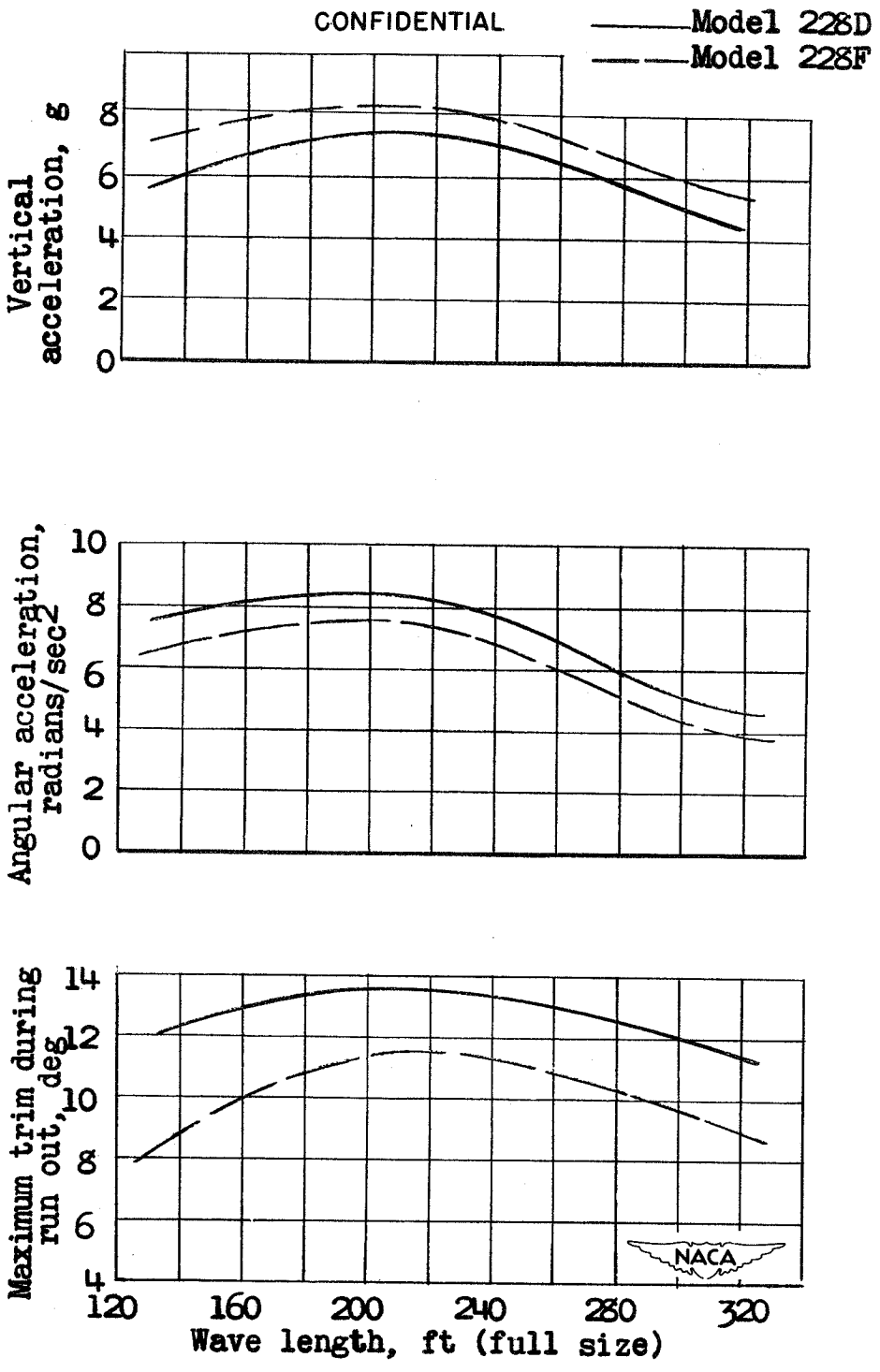

Figure 6.- Comparison of maximum accelerations and trims of models 228D and 228F.

CONFIDENTIAL

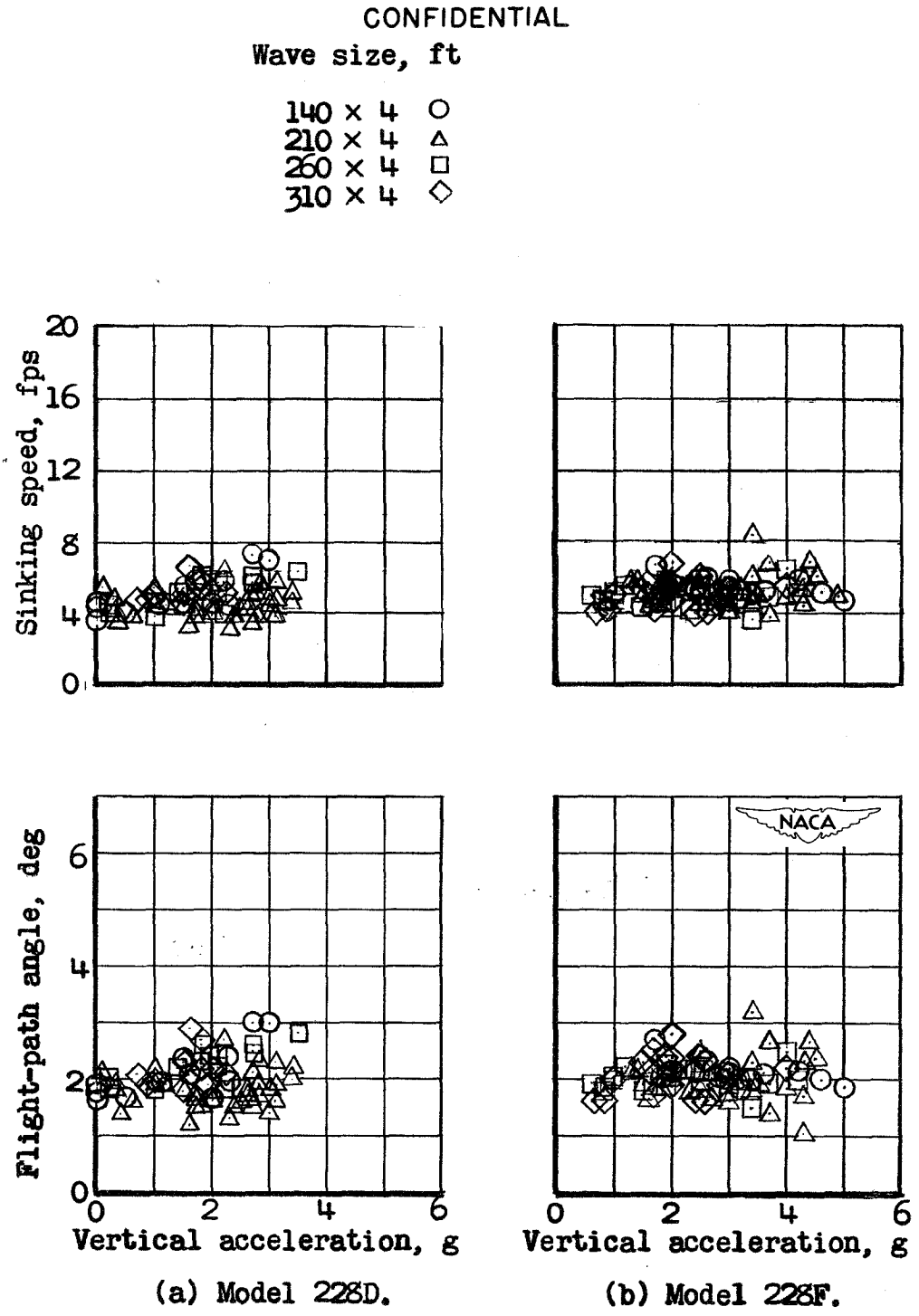

Figure 7.- Variation of sinking speed and flight-path angle at initial contact with vertical acceleration during initial impact.

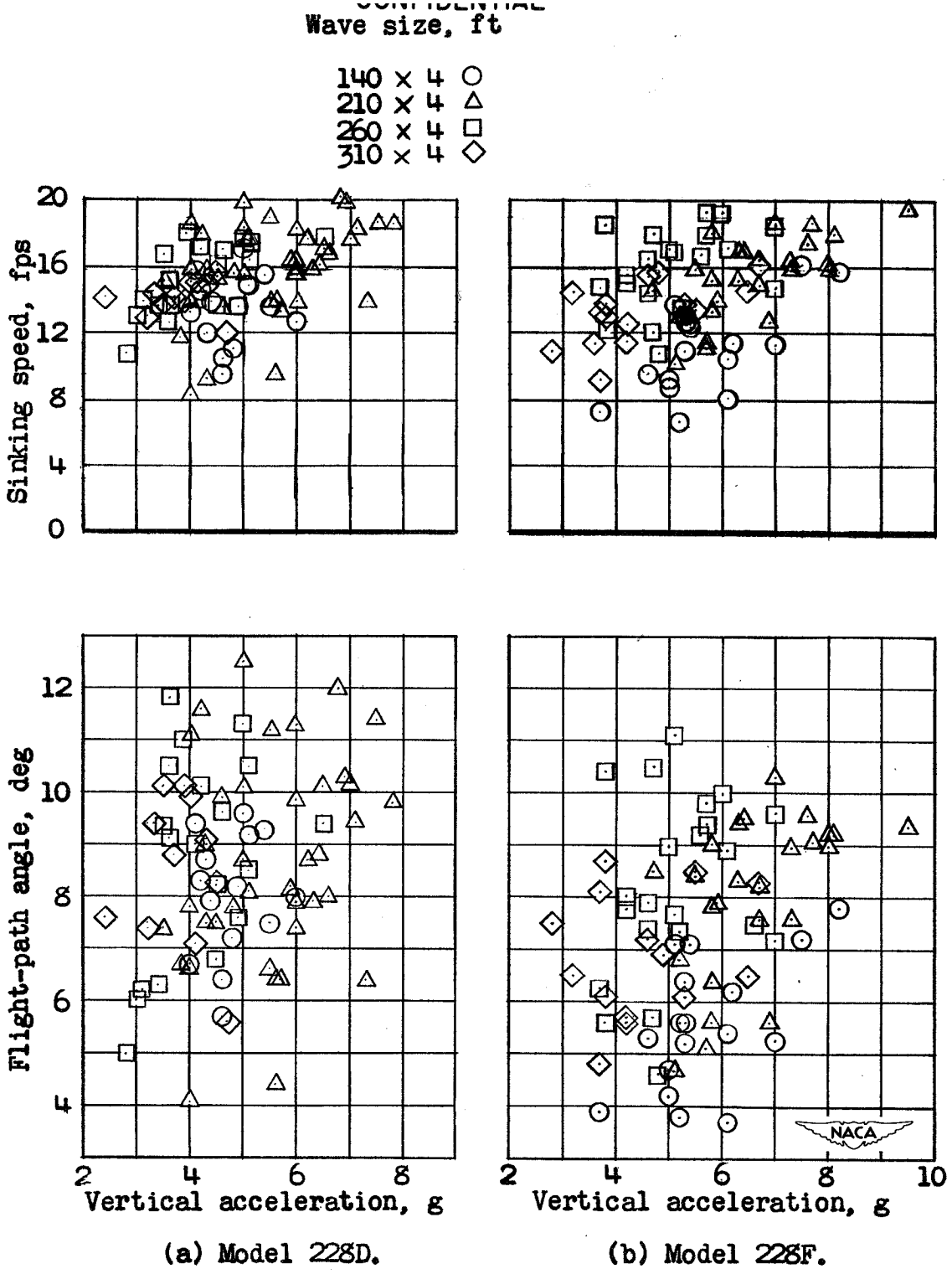

(a) Model 228D. (b) Model 228F.

Figure 8.- Sinking speed and flight-path angle at time of maximum vertical acceleration during landing run-out.